J. Mol. Biol. (1997) **272**, 106–120

JMB

Modelling Protein Docking using Shape Complementarity, Electrostatics and Biochemical Information

Henry A. Gabb, Richard M. Jackson and Michael J. E. Sternberg*

Biomolecular Modelling Laboratory, Imperial Cancer Research Fund, Lincoln's Inn Fields, P.O. Box 123, London WC2A 3PX, UK

**Corresponding author*

A protein docking study was performed for two classes of biomolecular complexes: six enzyme/inhibitor and four antibody/antigen. Biomolecular complexes for which crystal structures of both the complexed and uncomplexed proteins are available were used for eight of the ten test systems. Our docking experiments consist of a global search of translational and rotational space followed by refinement of the best predictions. Potential complexes are scored on the basis of shape complementarity and favourable electrostatic interactions using Fourier correlation theory. Since proteins undergo conformational changes upon binding, the scoring function must be sufficiently soft to dock unbound structures successfully. Some degree of surface overlap is tolerated to account for side-chain flexibility. Similarly for electrostatics, the interaction of the dispersed point charges of one protein with the Coulombic field of the other is measured rather than precise atomic interactions. We tested our docking protocol using the native rather than the complexed forms of the proteins to address the more scientifically interesting problem of predictive docking. In all but one of our test cases, correctly docked geometries (interface C^{α} RMS deviation $\leqslant 2$ Å from the experimental structure) are found during a global search of translational and rotational space in a list that was always less than 250 complexes and often less than 30. Varying degrees of biochemical information are still necessary to remove most of the incorrectly docked complexes.

Keywords: molecular recognition; protein–protein docking; protein–protein complex; predictive docking algorithm; fast Fourier transform

Introduction

Knowledge of the three-dimensional (3D) structure of protein–protein complexes provides a valuable understanding of the function of molecular systems. The rate of protein structure determination is increasing rapidly. Today there are some 5,000 entries in the Brookhaven Protein Data Bank (PDB) (Bernstein *et al*., 1977). However, determination of the structure of protein–protein complexes still remains a difficult problem with only about 100 deposited co-ordinates. Thus, computer algorithms capable of predicting protein–protein interactions are becoming increasingly important. Such algorithms can also provide insight into the process of protein–protein recognition.

The general strategy for simulating protein–protein docking involves matching shape complementarity (for recent reviews, see Janin, 1995a; Shoichet & Kuntz, 1996). Some approaches focus specifically on matching surfaces (e.g. see Jiang & Kim, 1991; Katchalski-Katzir *et al*., 1992; Walls & Sternberg, 1992; Helmer-Citterich & Tramontano, 1994). Others enhance the search for geometric complimentarity by matching the position of surface spheres and surface normals (e.g. see Kuntz *et al*., 1982; Shoichet & Kuntz, 1991; Norel *et al*., 1995). Shape complementarity is measured by a variety of scoring functions, some of which aim to model the hydrophobic effect during association from the change in solvent-accessible surface area of mol-

Abbreviations used: PDB, Brookhaven Protein Data Bank; 3D, three-dimensional; FFT, fast Fourier transform; DFT, discrete Fourier transform; IFT, inverse Fourier transform; CDR, complementarity determining region; RMS, root-mean square; CPU, central processing unit.

0022–2836/97/360106–15 $25.00/0/mb971203

ecular surface area (e.g. see Cherfils *et al*., 1991). Several algorithms employ a simplified scheme to estimate electrostatic interactions (e.g. see Jian & Kim, 1991; Walls & Sternberg, 1992). In general the algorithms yield a limited set of favourable complexes, one or a few of which are close (typically 1 to 3 Å RMS) to the native structure. Recognizing this, several groups have additionally focused on screening the correct solution from the false positives by modeling the hydrophobic effect, electrostatic interactions and desolvation (Gilson & Honig, 1988; Vakser & Aflalo, 1994; Jackson & Sternberg, 1995; Weng *et al*., 1996). Most of the above studies have focused on rigid body docking. Recently, however, Monte Carlo simulations have been used to refine flexible side-chain positions after rigid body docking (Totrov & Abagyan, 1994).

In the development of these algorithms many workers demonstrate that the bound complex can be generated starting from the component bound molecules. Simulations on the pertinent biological problem of docking starting from unbound complexes have also been performed on a limited number of test cases. However, these studies tended to be applications of algorithms developed on bound complexes. As a consequence, selective pruning of some interface side-chains was required to demonstrate that the algorithms could be applied to unbound complexes. The next step, therefore, is to establish an automated procedure that is successful on a series of molecules without manual intervention guided by knowledge of the answer.

An important step in the identification of reliable docking approaches was the blind trial organized by James and co-workers (Strynadka *et al*., 1996). Five groups submitted entries to predict the docking of β-lactamase and its inhibitor starting with the unbound structures prior to knowledge of the complex. All entrants were able to identify a solution close to the correct answer (i.e. better than 2.7 Å RMS for superposition of the predicted on the X-ray complex). The closest agreement was by Fourier correlation algorithm (Katchalski-Katzir *et al*., 1992), which found a 1.1 Å solution. This approach performs a complete translational and rotational search in Fourier space and selects binding geometries with high surface correlation scores. However, general conclusions cannot be drawn from one trial, particularly as the β-lactamase/inhibitor complex is highly amenable to docking methods that rely on shape complementarity alone as the surface area buried in the complex is particularly large (Janin, 1995a). It is not clear whether the Fourier approach or the other strategies involving measures of surface complementarity will reliably predict unbound systems without consideration of other properties, particularly electrostatics.

This paper reports extensive trials of docking unbound protein–protein molecules to obtain structural models for their complexes. Our approach recognises that a major problem in rigid body docking, starting with unbound complexes, is that the algorithm must be sufficiently soft to manage conformational changes, yet specific enough to identify the correct solution. At present, the alternative approaches of an initial non-rigid body search is computationally intractable. A variation of the Fourier correlation algorithm (Katchalski-Katzir *et al*., 1992) was chosen as it incorporates soft docking, is computationally fast and mathematically elegant. We introduce a soft treatment of electrostatic interactions into the Fourier correlation approach. In addition, we evaluate the selectivity provided by specific biological constraints of the type likely to be available in genuine docking applications.

Algorithm

Measuring shape complementarity by Fourier correlation

The docking protocol used in this study follows closely the shape recognition algorithm of Katchalski-Katzir *et al*. (1992) (shown schematically in Figure 1). The geometric surface recognition method takes advantage of the fast Fourier transform (FFT) and Fourier correlation theory to scan rapidly the translational space of two rigidly rotating molecules. The algorithm begins by discretizing two-molecules, A and B, in 3D grids with every node ($l,m,n = \{1 \ldots N\}$) assigned a value:

$$f_{A_{l,m,n}} = \begin{cases} 1 & : \quad \text{surface of molecule} \\ \rho & : \quad \text{core of molecule} \\ 0 & : \quad \text{open space} \end{cases}$$

and

$$f_{B_{l,m,n}} = \begin{cases} 1 & : \quad \text{inside molecule} \\ 0 & : \quad \text{open space} \end{cases}$$

By convention, *A* and *B* denote the larger and smaller proteins, respectively. Any grid node within 1.8 Å of an atom is considered to be inside a protein. Grid nodes at the surface of molecule A are scored differently. A 1.5 Å surface layer is used. We set $\rho = -15$ in all of our docking experiments. Contrary to the finding of Katchalski-Katzir *et al*.(1992) we find that the choice of ρ does affect the performance of the algorithm. Specifically, the degree of surface overlap tolerated during docking is directly related to the value of ρ.

In all our calculations, $128 \times 128 \times 128$ grids are used. Grid spacing is determined by the size of the respective molecules. The approximate radius of a protein is the distance between the geometric centre and the most distal atom. The grid size is the sum of the protein diameters plus 1 Å. Grid spacings ranged from 0.74 Å/node to 0.84 Å/node for the enzyme/inhibitor complexes and from 0.91 Å/node to 0.94 Å/node for the antibody/antigen complexes.

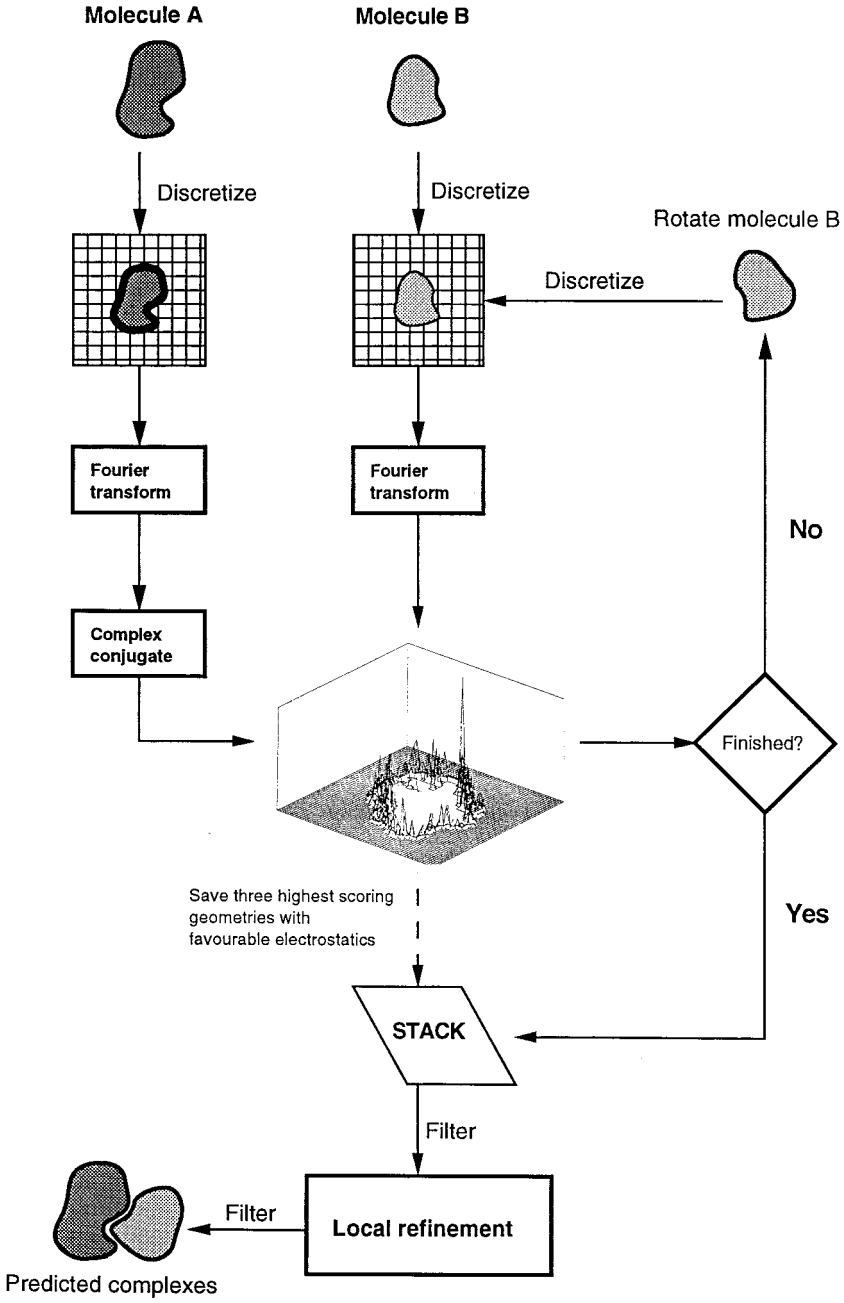

Figure 1. The Fourier correlation docking algorithm used in this study, based on the method of Katchalski-Katzir *et al*. (1992). Molecules A and B are discretized differently. Molecule A has a negative core and a positive surface layer (the dark band) whereas no surface core distinction is made for molecule B. It is only necessary to discretize and Fourier transform molecule A one time. Electrostatic complementarity is calculated concurrently with shape complementarity. Similarly, the transform of the electric field of molecule A need only be calculated once. The cross-section of a sample 3D Fourier correlation function illustrates a search of translational space. The geometric centres of the two molecules are superposed at the origin. Molecule A is fixed in the centre of the grid. As molecule B moves through the grid, a ''signal'' describing shape complementarity emerges. A zero correlation score indicates that the proteins are not in contact while negative scores (the empty region in the centre) indicate significant surface penetration. The highest peak indicates the translation vector giving the best surface complementarity.

The correlation function of f_A and f_B is:

$$f_{C_{\alpha,\beta,\gamma}} = \sum_{l=1}^{N} \sum_{m=1}^{N} \sum_{n=1}^{N} f_{A_{l,m,n}} \times f_{B_{l+\alpha,m+\beta,n+\gamma}}$$

where N^3 is the number of grid points and α, β, γ is the translation vector of molecule B relative to A. A high correlation score denotes a complex with good surface complementarity. If molecule B significantly overlaps molecule A the correlation is negative. Zero correlation most likely means that the molecules are not in contact.

Calculating $f_{C_{l,m,n}}$ as shown above is very inefficient, requiring N^3 multiplications and additions for every N^3 shifts α, β, γ. Since f_A and f_B are discrete functions i.e. (representing the discretized molecules) it is possible to calculate f_C much more rapidly by FFT. The FFT requires of the order of N^3 ln (N^3) calculations, which is significantly less than N^6. (See Press *et al*. (1986) and Bracewell (1990) for thorough reviews of fast transforms and Fourier correlation.) The discrete functions f_A and f_B are transformed (denoted DFT for discrete Fourier transform) and the complex conjugate $F_A^*$is multiplied times F_B:

$$F_A = \mathrm{DFT}(f_A)$$
$$F_B = \mathrm{DFT}(f_B)$$
$$F_C = (F_A^*)(F_B)$$

The correlation function describing the shape complementarity of molecules A and B along each

translational vector is the inverse Fourier transform (IFT) of the transform product:

$$f_C = \mathrm{IFT}(F_C)$$

A cross-section through a sample correlation function is shown in Figure 1. The highest peak denotes the translation vector producing the best shape complementarity for the current orientation.

After each translational scan, molecule B is rotated about one of its Euler angles until rotational space has been completely scanned. For an angular deviation of $\alpha = 15^\circ$, this yields $360 \times 360 \times 180/\alpha^3 = 6912$ orientations. However, many of these orientations are degenerate and must be removed using the following relationship (Lattman, 1972):

$$\alpha = \cos^{-1} \frac{\mathrm{tr}(R_1 \times R_2^T) - 1}{2}$$

where R_1 is the rotation matrix of the first orientation, R_2^T is the transpose of the rotation matrix of the second orientation, and tr is the matrix trace. If $\alpha \leqslant 1^\circ$ then the two orientations are degenerate. Removing degeneracies in this fashion yields 6385 unique orientations. A finer angular rotation is computationally demanding for extensive trials. For example, there are 22,105 non-degenerate orientations for $\alpha = 10^\circ$.

Measuring electrostatic complementarity by Fourier correlation

Shape complementarity is not the only factor involved in molecular binding. Electrostatic attraction, particularly the specific charge–charge interactions in the binding interface, also plays an important role. For speed and consistency, electrostatic complementarity is calculated by Fourier correlation using a simple Coulombic model. Since charged amino acid side-chains are usually on the protein surface, they are often involved in binding and tend to be highly flexible (Figure 2). Therefore, calculating individual point charge interactions when attempting to dock the uncomplexed structures is not feasible and can produce misleading results. So rather than try to measure specific charge–charge interactions, we measure the point charges of one protein interacting with the electric field of the other as grid points. In this way, point charges are dispersed to simulate side-chain movement. The electrostatic calculations proceed in a manner very similar to those of shape complementarity. Charges are assigned to the atoms of protein A (Table 1) and the molecule is placed in a grid. The electric field at each grid node (excluding those of the protein core) is calculated:

$$\phi_i = \sum_j \frac{q_j}{\varepsilon(r_{ij}) r_{ij}}$$

where ϕ_i, is the field strength at node i (position l,m,n), q_j is the charge on atom j,r_{ij} is the distance between i and j (a minimum cutoff distance of 2 Å is imposed to avoid artificially large values of ϕ), and $\varepsilon(r_{ij})$ is a distance-dependent dielectric function. In this case, a pseudo-sigmoidal function, based on the sigmoidal function of Hingerty *et al.* (1985), is used:

$$\varepsilon(r_{ij}) = \begin{cases} 4 & : \quad r_{ij} \leq 6 \text{ Å} \\ 38 r_{ij} - 224 & : \quad 6 \text{ Å} < r_{ij} < 8 \text{ Å} \\ 80 & : \quad r_{ij} \geq 8 \text{ Å} \end{cases}$$

Several distance-dependent dielectric functions were tested. This one was chosen because it effectively damps long-range electrostatic effects that are not relevant to the binding interface. In fact, dielectric functions that do not damp long-range effects give inconsistent results, sometimes showing poor electrostatics for experimentally determined complexes. The treatment of protein B is much simpler. Charges are assigned to its atoms and then

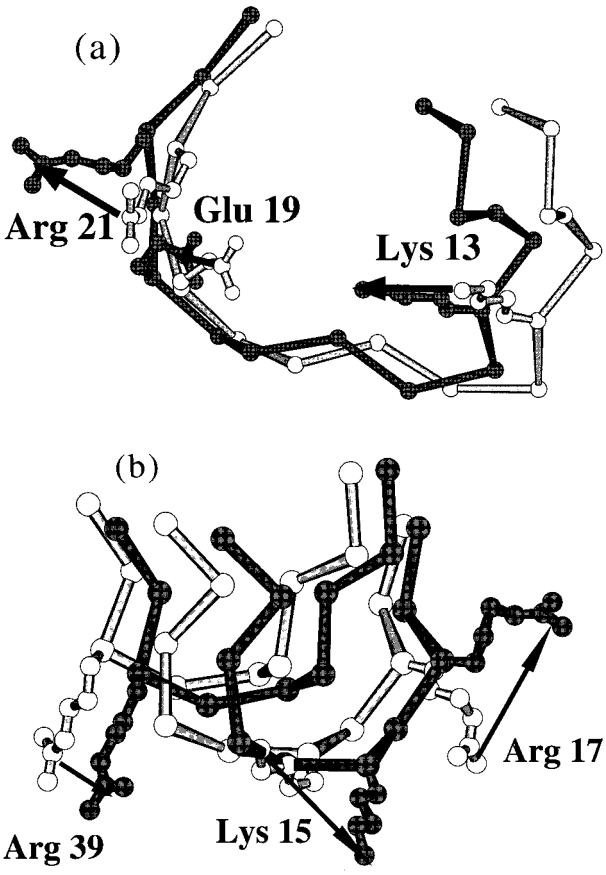

Figure 2. Examples of docking to illustrate induced binding in the interface. (a) Selected binding site residues of ovomucoid when free (2ovo, light grey) and when bound to α-chymotrypsin (1cho, dark grey). (b) Selected binding site residues of BPTI when free (4pti, light grey) and when bound to trypsin (2ptc, dark grey). Scoring functions used for predictive docking must be sufficiently ''soft'' to account for conformational changes of this magnitude. The whole complexes for CHO and PTC are shown in Figures 4(b) and (d) respectively.

Table 1. Charges used in Coulombic electrostatic fields

Peptide backbone	Charge	Side-chain atoms	Charge
Terminal-N	1.0	Arg-N^{η}	0.5
Terminal-O	−1.0	Glu-O^{ε}	−0.5
C^{α}	0.0	Asp-O^{δ}	−0.5
C	0.0	Lys-N^{ζ}	1.0
O	−0.5	Pro-N	−0.1
N	0.5		

discretized in a grid ($q_{l,m,n}$) by trilinear weighting (Rogers & Sternberg, 1984; Edmonds *et al.*, 1984).

Calculations of the electrostatic interactions proceeds as outlined in Figure 1 and as described for surface correlation except that the discrete functions are:

$$f_{A_{l,m,n}} = \begin{cases} \phi_{l,m,n} & : \text{ entire grid excluding core} \\ 0 & : \text{ core of molecule} \end{cases}$$

$$f_{B_{l,m,n}} = q_{l,m,n}$$

and the correlation function becomes:

$$f^{\text{elec}}_{\alpha,\beta,\gamma} = \sum_{l=1}^{N}\sum_{m=1}^{N}\sum_{n=1}^{N} \phi_{A_{l,m,n}} \times q_{B_{l+\alpha,m+\beta,n+\gamma}}$$

So both grids are Fourier transformed and correlated such that the static charges of molecule B move through the electric field of molecule A. The electrostatic correlation score is used as a binary filter. Specifically, false positive geometries that give high shape correlation scores can be excluded if their electrostatic correlation is unfavourable (i.e. positive).

Results

Predictive docking of native protein structures

The docking protocol, shown schematically in Figure 1, was applied to the unbound coordinates of six enzyme/inhibitor and two antibody/antigen systems. In addition, two bound antibodies were docked to unbound antigens. These ten systems are referred to as ''unbound'' docking, for simplicity. Docked solutions are ranked by surface correlation score. A correct solution is defined as any geometry with an interface C^{α} RMS less than or equal to 2.5 Å from the crystal structure (see Methods).

The results of the global search before filtering and without consideration of electrostatics show that geometric complementarity alone (as measured by Katchalski-Katzir *et al.*, 1992) cannot reliably dock unbound complexes (Tables 2 and 3). For three out of the ten test systems no correctly docked complex is ranked in the top 4000 predictions. For the other seven systems, the highest ranked correct answer was in a list of hundreds of alternatives. This shows that a high surface correlation score does not necessarily indicate a correctly docked complex. For example, even a limited rotational scan near the correct geometry produces a broad range of correlation scores (Figure 3). In a complete rotational search it is possible to find incorrectly docked complexes that score higher than the actual crystal structure. This does not pose a problem because our aim during the global search is to place at least one near-correct prediction in the final output; not necessarily at the highest scoring position. Correctly docked complexes can be screened later using experimental constraints and advanced refinement techniques.

The additional constraint of removing predictions with unfavourable electrostatic interactions markedly improves the ranking of correctly docked structures in the global search (Table 2). With electrostatics, a good solution is found in the top 4000 structures in nine out of ten systems. In general, inclusion of electrostatics reduces the number of geometries to be evaluated by approximately 50%.

Global searching and the dependence on filtering

Knowledge of the location of the binding site on one, or both proteins drastically reduces the number of possible allowed conformations. Knowing specific binding site residues reduces the search space even further. It is possible to utilize this information in the form of distance constraints (see Methods). Generally, information about the binding site is available from experimental data (e.g. site-directed mutagenesis, chemical cross-linking, phylogenetic data). In the absence of experimental data, it is often possible to predict the correct binding site by examining potential hydrogen bonding groups, clefts and/or charged sites on a protein surface (Gilson & Honig, 1987; DesJarlais *et al.*, 1988; Nicholls & Honig 1991; Laskowski, 1995; Laskowski *et al.*, 1996; Meyer *et al.*, 1996). Serine proteases and immunoglobulins represent systems where the binding sites are known in advance. The catalytic triad of the serine proteases and the complementarity determining region (CDR) of immunoglobulins are both well characterized. We take advantage of this information to varying degrees in our docking experiments (Table 2). In the serine protease/inhibitor docking attempts, filters are defined as: loose, any residue of the inhibitor in contact with any residue of the catalytic triad (i.e. His, Asp, Ser); medium, an inhibitor residue in contact with both the His and the Ser of the catalytic triad; tight, a specific binding site residue of the inhibitor in contact with both the His and the Ser of the catalytic triad. In the antibody/lysozyme docking attempts, filters are defined as: loose, any part of the lysozyme in contact with either the L3 or the H3 CDR; medium, lysozyme in contact with both the L3 and H3 CDRs; tight, the medium filter together with one residue of the epitope in contact with any part of the CDR. The L3/H3 CDR filters are based on the study of MacCullum *et al.* (1996), which

Table 2. Docking unbound subunits with varying degrees of filtering

	Global search											
	Before filtering			Loose filtering			Medium filtering			Tight filtering		
	Rank ($N = 4000$)											
	No elec	Elec	$N \leqslant 2.5$ Å	N	Rank	$N \leqslant 2.5$ Å	N	Rank	$N \leqslant 2.5$ Å	N	Rank	$N \leqslant 2.5$ Å
CGI	207	87	2	172	5	2	24	2	1	7	1	1
CHO	282	127	7	234	12	7	19	2	7	13	1	7
KAI	462	223	25	377	64	19	85	45	13	48	27	13
PTC	989	502	8	242	39	8	34	3	8	21	2	8
SNI	NF	1518	2	29	19	2	3	2	2	2	1	2
SIC	NF	NF	0	–	–	–	–	–	–	–	–	–
FDL	219	106	2	717	22	2	331	14	2	51	3	2
MLC	188	104	5	623	13	5	97	3	5	20	1	5
HFL	NF	3318	2	544	460	2	16	13	2	6	5	2
HFM	100	67	7	837	27	7	177	5	5	40	1	5

N, the number of predictions remaining at each stage. Rank refers to the position of the first correct answer in the list of predictions. NF, none found. $N \leqslant 2.5$ Å equals the number of predicted complexes with an interface C^{α} RMS $\leqslant 2.5$ Å.

The following side-chain lengths were used during filtering: Gly, 0.5 Å; Ala, Thr, Val, 1.0 Å; Cys, Ile, Leu, Ser, 2.0 Å; Asn, Asp, Pro, 3.0 Å; Gly, Glu, His, Met, Phe, 4.0 Å; Lys, Trp, Tyr, 5.0 Å; Arg, 6.0 Å

analysed general structural principles of antibody/antigen contacts.

If the proteins in question are heavily studied, as are serine proteases and immunoglobulins, information typical of the medium or the tight filter might be available. In other practical applications of docking, there often will be some available constraints typical of the loose filter. Table 2 shows that loose filtering of the output from the global search removes between 79 and 99% of false positives, usually leaving at least one correct answer in the top 50 predictions. As expected, medium and tight filtering removes successively more incorrect predictions. For example, going from loose to medium filtering reduces the total number of predictions by an order of magnitude. With fewer false positives to contend with, the ranking of the correct predictions improves dramatically. A good solution is in the top five in six out of nine cases. For the other three systems no more than 45 alternate geometries would have to be examined. In going from medium to tight filtering, although the procedure does not significantly alter the number of false positives, a near correct geometry is ranked in the top five predictions in all but two of the nine test systems. In one other system, the good solution is rank 27. It is clear that given experimental constraints this docking procedure can effectively dock two proteins using crystal structures for the unbound subunits. Since few predictions remain at this stage, it may be possible to use more computationally demanding, and hence more accurate models to predict binding.

Local refinement of predicted geometries

The global search is carried out at an angular deviation of $\alpha = 15^{\circ}$. A finer rotational scan is desirable but computationally expensive. So, a local refinement of the most reasonable predictions is performed. We chose to refine the structures that passed through the loose filter because this level of information is generally available, e.g. in the docking challenge (Strynadka *et al.*, 1996). During refinement each geometry is shifted (±5 Å in each direction) and rotated (±5° for each Euler angle) slightly to find the highest surface correlation score in the local space. Refinement using the same surface thickness as in the global search (1.5 Å) did not improve selectivity as evaluated by the rank of the first good solution; in some systems ranking was improved but in others it was worse. How-

Table 3. Docking unbound subunits: global search and local refinement

	Filtered global search				Local refinement (1.5 Å surface)				Local refinement (1.2 Å surface)			
	N	Rank	$N \leqslant 2.5$ Å	C^{α} RMS	N	Rank	$N \leqslant 2.5$ Å	C^{α} RMS	N	Rank	$N \leqslant 2.5$ Å	C^{α} RMS
CGI	172	5	2	2.1/1.9	94	3	1	1.8/2.0	133	1	1	1.7/2.0
CHO	234	12	7	1.4/1.3	86	11	5	1.2/1.1	178	8	6	1.5/1.7
KAI	377	64	19	2.2/1.8	364	130	18	1.5/1.2	181	33	4	1.9/1.6
PTC	242	39	8	1.9/2.0	229	16	8	1.5/1.7	177	9	7	1.7/1.6
SNI	29	19	2	1.8/1.6	26	8	2	1.8/1.6	15	2	1	2.4/1.9
SIC	–	–	–	–/–	–	–	–	–/–	–	–	–	–/–
FDL	717	22	2	2.1/1.8	707	176	2	2.1/1.8	525	–	–	–/–
MLC	623	13	5	2.2/1.9	590	41	4	1.2/1.6	378	1	4	2.0/2.1
HFL	544	460	2	2.3/1.8	519	228	2	1.8/1.5	403	78	2	1.5/1.5
HFM	837	27	7	1.7/1.5	762	65	6	1.1/1.1	408	1	2	0.7/0.8

C^{α} RMS no./no. refers to the total C^{α} RMS and the interface C^{α} RMS, respectively.

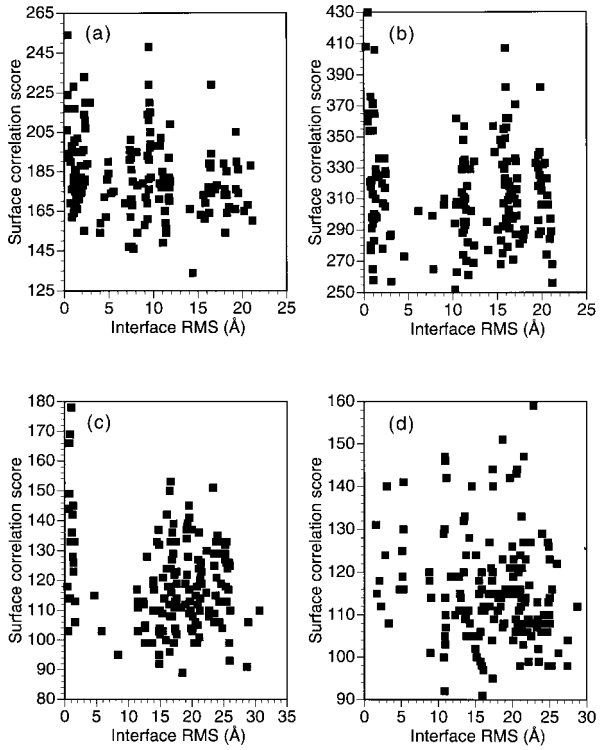

Figure 3. A high surface correlation score does not necessarily indicate a correct complex. Limited rotational scans (±15° in 5° increments for each Euler angle) around the correct geometry were performed using the bound and unbound structures of KAI and MLC: (a) complexed KAI structures, (b) native KAI structures (2/pka/1bpi), (c) complexed MLC structures (1mlc), (d) native MLC structures (1cfa/1lza). These plots show that high surface correlation scores are possible for incorrect geometries and *vice versa*.

ever, refinement tends to improve the final RMS values of the highest ranked correct predictions for the enzyme/inhibitor complexes (exception: KAI; Table 3). Refining the antibody/antigen predictions proved more difficult. In each case except HFL, refinement of the filtered data from the global search worsened the rank of the first correctly docked complex. HFL, however, had the worst overall rank.

To improve these results, we performed the refinement again using a thinner surface thickness (1.2 Å). A thinner surface layer is less tolerant of overlapping protein surfaces. This leads to more stringent scoring of shape complementarity, something that is not necessarily beneficial when doing a global search of docking space for native structures. However, stricter shape fitting tends to dampen correlation scores for false positives while enhancing those of predicted complexes already near the correct docking geometry, as shown in Table 3. With the exception of FDL, using a slightly thinner surface thickness significantly improves ranking but sometimes worsens RMS. This suggests that there is not strict correlation between surface complementarity score and the correct RMS when docking native structures (Figure 3).

Enzyme/inhibitor docking

The highest ranked correct prediction for each enzyme/inhibitor test case after refinement (1.5 Å surface thickness) is shown in Figure 4. Note that these are not necessarily the predictions with the best RMS values. CGI represents the best of all our docking attempts. A correct answer scores in the top 100 predictions after the global search. Loose filtering leaves a reasonable number of complexes for subsequent refinement, after which a correct answer is ranked in the top five regardless of the surface thickness used (Table 3). The single remaining correct structure is shown in Figure 4(a). Inspection shows that the RMS deviation from the correct docking geometry is primarily rotational.

CHO represents another successful docking attempt. Loose filtering and local refinement leave several correct geometries, one of which is the top 20 predictions (Table 3). The deviation from the crystal structure of the complex is primarily rotational but with a small translational component as well (Figure 4(b)).

Problems arose during the refinement of KAI. Unlike the other enzyme/inhibitor test cases, refinement using a 1.5 Å surface layer worsened the rank of the best prediction while improving its RMS deviation (Table 3), which is primarily rotational (Figure 4c). Results were better when a thinner surface thickness was used; both the rank and RMS values improved.

The attempt by Katchalski-Katzir *et al.* (1992) to dock trypsin and BPTI was unsuccessful, leading the authors to conclude that docking native structures was beyond the capability of the Fourier correlation algorithm. We also find that PTC is a difficult test case. Even with the added electrostatic filtering (not available in the original work of Katchalski-Katzir and co-workers) the first correct prediction still ranks far down in the list of possibilities (Table 3). All of the structures used in this study experience some induced binding effects, but compared to the binding site of ovomucoid (Figure 2(a)), for example, the amino acid side-chains of BPTI that are important to binding, especially Lys15, undergo significant conformational change upon binding to trypsin (Figure 2(b)). Loose filtering, however, reduces the global search to more manageable proportions, leaving several correct geometries, including one in the top 50 predictions. Subsequent refinement improves both rank and RMS (Table 3). The RMS deviation is almost entirely translational (Figure 4(d)).

Similar to PTC, SNI is another case where electrostatic filtering and at least some experimental data are essential if a correctly docked complex is to be found at all. However, applying the loose filter removes 99% of the false positives. Refinement at either surface thickness improves the final rank-

ings but not the RMS values. The RMS deviation is mostly translational but with a small rotational component (Figure 4(e)).

SIC is the only case in which no correct answers were found in the top 4000 predictions. The first correct answer is found at rank 7745. The docking was performed again but with all side-chains greater than 70% solvent-exposed truncated at the c^{γ} position. This time, correctly docked structures scored in the top 1000 predictions. However, this does not represent a general solution to the docking problem, since truncating exposed side-chains worsened results for the other test cases (data not shown).

Grid resolutions for the enzyme/inhibitor test cases are: CGI, 0.78; CHO, 0.76; KAI, 0.74; PTC,

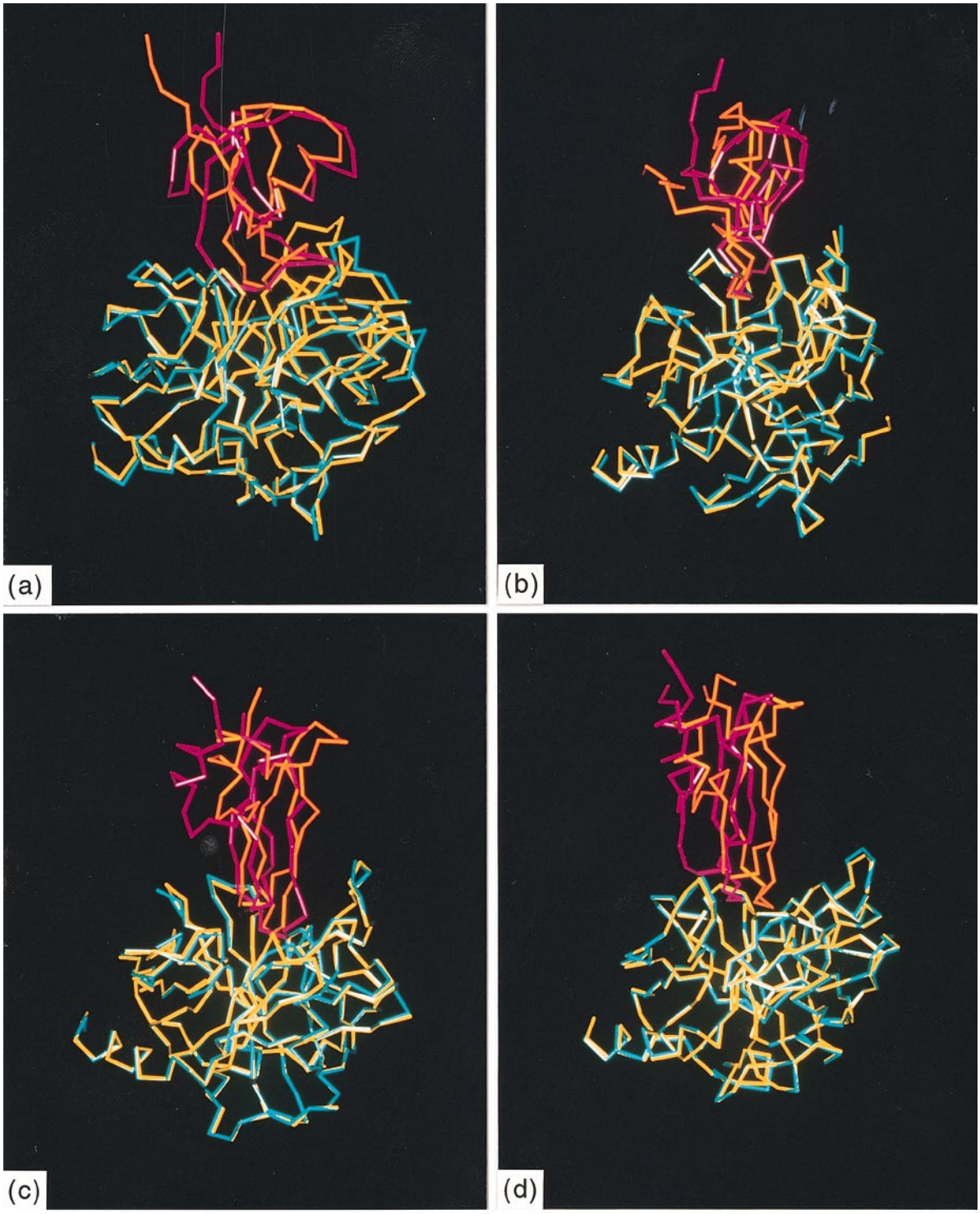

Figure 4(a–d) (*legend on page 114*)

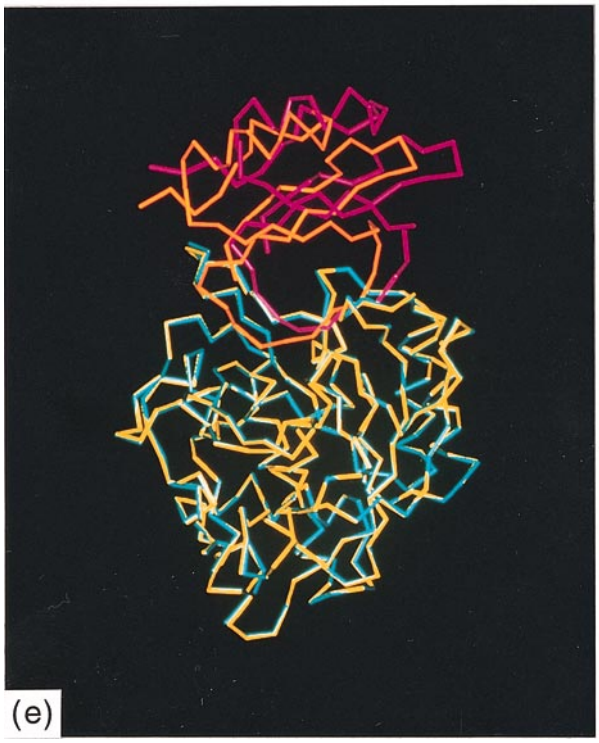

Figure 4. The highest ranked predicted geometries for the enzyme/inhibitor test cases superposed onto the crystal structure of the enzyme (a) CGI, (b) CHO, (c) KAI, (d) PTC, (e) SNI. In each case, the view was chosen to highlight the difference between the correctly bound antigen and the prediction. The crystal structure of the inhibitor/enzyme complex is shown in orange/yellow and the predicted docking in magenta/cyan.

0.76; SNI, 0.78; and SIC, 0.84 Å/grid space. It is tempting to blame the failure to dock SIC on the comparatively large grid spacing. However, antibody/antigen complexes require even larger grid spacings: FDL, 0.96; MLC, 0.91; HFL, 0.94; and HFM, 0.94 Å/grid space. In general, the docking results for both sets of molecules are qualitatively similar, suggesting that the failure of SIC is not a consequence of grid resolution.

Antibody/antigen docking

The highest ranked correct prediction for each antibody/antigen test case after refinement (1.5 Å surface thickness) is shown in Figure 5. FDL is the most difficult of the antibody docking tests (Figure 5(a)). Our refinement scheme failed to improve either the rank of the first correct prediction or its RMS values. Near the interface, the RMS difference from the crystal structure is primarily translational. Further from the interface, the rotational component of the RMS difference becomes more apparent. The highest ranked, refined prediction for MLC is shown in Figure 5(b). The RMS deviation from the crystal structure is primarily translational.

Since the free antibodies for HFL and HFM have not been solved crystallographically, it was necessary to use the complexed forms of the F_vs. Refinement of HFL improved both the rank and RMS of the first correctly predicted complex. The rank, however, was still lower than the other antibody/antigen test cases in spite of the fact that the bound form of the antibody was used. The RMS difference for HFL is mostly rotational and for the most part away from the interface, which is in close agreement with the crystal structure (Figure 5(c)). HFM represents the best of the antibody/antigen docking attempts in terms of rank and RMS (Table 3). The RMS difference from the crystal structure is primarily translational with a slight rotational component visible further from the interface (Figure 5(d)).

Docking complexed protein structures

The test systems used in this study were chosen because crystal structures were available for both the free and complexed subunits. We decided to test our docking procedure on bound conformers using the same parameter set as used to dock the unbound proteins. To avoid biasing towards the original binding orientation, the subunits of the complexes are rotated at random before starting the global search. As expected, better results are obtained when docking bound conformers (Table 4) compared to native structures (Tables 2 and 3). In general, a correct answer ranks in the top 100 predictions after the global search. Electrostatic filtering improves the ranking of correct geometries by, roughly, a factor of 2, similar to the results for unbound docking (Table 2). However, even in the absence of electrostatics the results are fairly good. In two cases, SIC and FDL, however, electrostatics is essential in order to score a correct answer in the top 4000 predictions. There are also a greater number of correctly docked predictions in the final output from the global search, more so for the enzyme/inhibitor than for the antibody/antigen complexes.

Local refinement consistently improves the final RMS values of the highest scoring correct prediction. However, in all but three cases the final rank of this structure is worsened. Using the electrostatic filter during local refinement does not significantly change this result (not shown). It should be noted that the docking parameters were optimized for unbound molecules where shape complementarity is less specific. So improved performance using bound molecules is not necessarily to be expected. Still, the overall results of docking using bound conformers is superior to predictive docking using native structures. A correctly docked complex is consistently placed in the top 100 scoring geometries with an overall greater density of correct answers in the final output. This highlights the

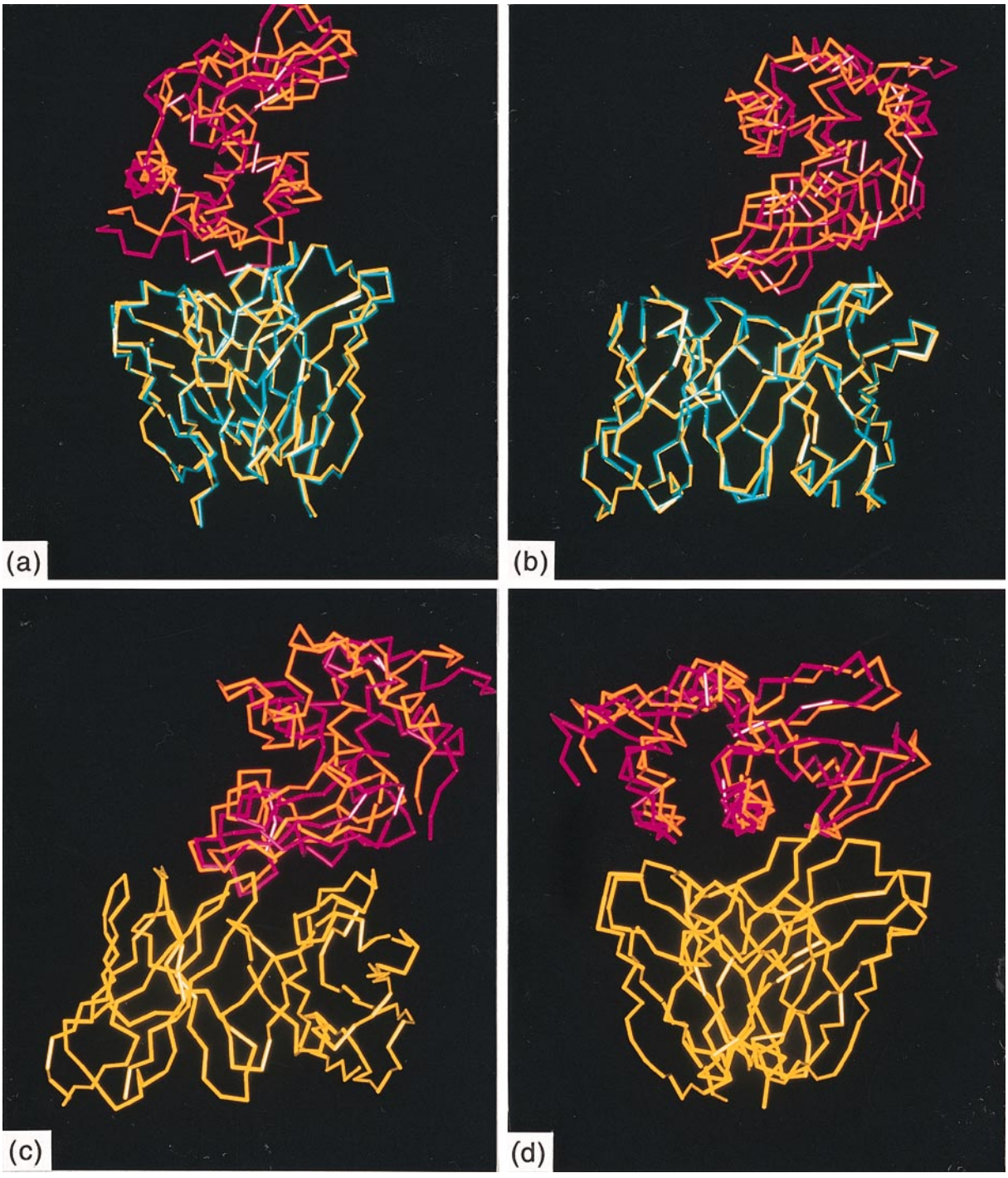

Figure 5. The highest ranked predicted geometries for the antibody/antigen test systems superposed on the crystal structure of the F_v (a) FDL, (b) MLC, (c) HFL, (d) HFM. The view was chosen to highlight the difference between the correctly bound antigen and the prediction. The crystal structure of the lysozyme/antibody complex is shown in orange/yellow and the predicted docking in magenta/cyan.

Table 4. Docking native structures

	Global search			Loose filtered global search				Local refinement (1.5 Å surface)			
	Rank ($N = 4000$)										
	No elec	Elec	$N \leqslant 2.5$ Å	N	Rank	$N \leqslant 2.5$ Å	C^{α} RMS	N	Rank	$N \leqslant 2.5$ Å	C^{α} RMS
CGI	87	45	19	174	3	19	1.8/1.7	161	3	19	1.0/1.0
CHO	118	59	15	238	3	13	1.6/1.6	218	40	13	0.8/0.9
KAI	33	25	30	534	25	30	1.4/1.3	502	38	28	0.4/0.4
PTC	232	118	6	515	24	6	0.8/0.8	513	91	7	0.7/0.8
SNI	104	40	15	62	2	15	0.6/0.7	54	8	15	0.6/0.7
SIC	NF	985	2	37	8	2	1.2/1.1	30	22	2	0.8/0.7
FDL	NF	1983	1	644	355	1	0.6/0.8	631	240	1	0.7/0.8
MLC	52	23	8	522	5	8	0.6/0.7	507	2	8	0.8/0.8
HFL	158	89	7	805	16	7	0.7/0.8	784	96	7	0.8/0.9
HFM	118	78	2	664	23	2	0.8/0.9	633	104	2	0.8/0.9

problem of evaluating docking protocols using bound complexes.

Discussion and Conclusions

We have presented a docking protocol based on the Fourier correlation algorithm (Katchalski-Katzir *et al.*, 1992). Our method used a parameter set developed specifically for docking native structures and therefore can be used for predictive docking. In addition, a simple but effective treatment of electrostatic interactions further improved our ability to distinguish true from false positive dockings. Because of this we were able to succeed in at least one test system where surface correlation alone failed. A complete search of translational and rotational space is performed, but within this space the correct binding geometry is quite small, so most of the complexes sampled are incorrect by definition. This leads to noisy output. Even after post-filtering based on experimental data there are significantly more incorrectly docked structures than correct solutions. Though the present combination of surface omplementarity and electrostatic interactions performs well for native structures, experimental information in the form of distance constraints is necessary in order to separate correct solutions from false positives. Three levels of filter were applied to the output, each with successively more information about the binding interface, and each producing successively better results (Table 2).

Since protein–protein binding is governed, among other things, by electrostatic interactions as well as hydrophobicity, one cannot expect surface complementarity alone to distinguish true from false positives in predictive docking. Hydrophobicity is modelled implicitly in the surface complementarity score (e.g. see Cherfils *et al.*, 1991; Jackson & Sternberg, 1995) but electrostatic interactions were not included in the original Fourier correlation method (Katchalski-Katzir *et al.*, 1992). We decided to consider electrostatics with the aim of excluding false positives and improving the rank of the correct answers. We opted for a simple Coulombic model rather than a more rigorous, and more computationally expensive, Poisson–Boltzmann description (Warwicker & Watson, 1982; Sharp & Honig, 1990). A dispersed Coulombic field was used rather than charge–charge interactions described at atomic level. Point charge interactions failed to distinguish right from wrong answers (data not shown) for the simple reason that the side-chains governing specificity are not necessarily in their optimal binding conformations. Individual charges will rarely be positioned for favorable interaction. In fact, they can often be placed in a repulsive interaction even if the backbone geometry is correct. Even one unrealistically close contact can severely distort the electrostatic calculations. A Coulombic field, whose absolute value has an upper bound, disperses the charges in a manner that simulates the uncertainty in side-chain conformation. It is therefore sufficiently ''soft'' to dock native structures. However, at this level of detail, electrostatics can only be used as a binary filter as it is not sufficiently sensitive to be included directly in the scoring function. However, the results show that removing predictions with unfavorable electrostatics significantly improves the ranking of correctly docked complexes (Table 2). In some complexes, it is essential in order to find any correct answers.

Other researchers have used lower-resolution grids and coarser rotational scans for their initial search (Katchalski-Katzir *et al.*, 1992; Vakser & Aflalo, 1994; Meyer *et al.*, 1996) Vakser & Aflalo (1994), for example, used a $64 \times 64 \times 64$ grid. In our initial studies, we used a $64 \times 64 \times 64$ grid with an angular deviation of 20° for our global search. This produced marginal results for the enzyme/inhibitor systems but failed to find correct solutions for the antibody/antigen systems (data not shown). Antibody/antigen systems are too large to model at this grid resolution and angular deviation. Access to a more powerful computer capable of performing the FFT in parallel enabled us to rapidly perform both stages of docking (i.e. global search and local refinement) at high resolution. This significantly improved our results for both enzyme/inhibitor and antibody/antigen docking.

We obtained good results using a surface layer that was thinner than that normally used by other groups. In docking the challenge, for example, Eisenstein and co-workers were successful using a

surface thickness of 3.5 Å (Strynadka *et al*., 1996). However, using the bound forms of the proteins studied in this paper, we saw very little shape complementarity when using a thicker surface layer in the procedure (data not shown). The final output was composed primarily of complexes that buried large amounts of surface area with substantial overlap with the protein core. A thinner surface layer demands greater shape specificity and our results show that a surface thickness of 1.5 Å works well when docking unbound proteins. Decreasing surface thickness to 1.2 Å during local refinement improved results even further (Table 3). Local refinement using the same surface thickness (i.e. 1.5 Å) as the global search is less able to distinguish correctly docked molecules clearly (Table 3). This suggests that a sufficient level of surface complementarity still exists at the protein–protein interface in spite of incorrectly positioned side-chains.

It has been suggested that enzyme/inhibitor and antibody/antigen complexes represent two different classes of binding (Lawrence & Colman, 1993). Enzymes and their inhibitors have co-evolved to form an interface with a high degree of surface complementarity. On the other hand, the immune system produces many different antibodies in response to an antigen, some of which bind their respective epitopes quite well while others bind quite poorly. So a particular antibody/antigen complex does not necessarily possess the best possible binding interface. Shape correlation may not be as important in antibody/antigen complexes (Lawrence & Colman, 1993). Our results for the bound forms do show slightly better surface complementarity for the enzyme/inhibitor complexes than for the antibody/antigen complexes. This may reflect the different classes of binding. Perhaps it is not a coincidence that the β-lactamase/inhibitor complex was predicted successfully by all research groups in the first docking challenge (Strynadka *et al*., 1996) whereas no groups could dock an antibody to haemagglutinin in the second docking challenge (Dunbrack *et al*., 1997).

Protein docking algorithms can provide insights into the kinetics and stability of recognition (e.g. see Janin, 1995b). Our procedure does not consider association at the atomic level and thus it is inappropriate to interpret the results in terms of individual atomic interactions. However, the global search followed by local refinement could mimic aspects of molecular recognition. Our treatment considers geometric and electrostatic complementarity at a lower resolution. This level of detail may well model a state in which the two proteins are close to their native conformation but the precise atomic interactions have not been achieved. Such a state might be similar to the molten globule phase during protein folding (Ptitsyn, 1995). This study shows that there are a very limited number of orientations by which an optimised binding interface can associate with an active site or an antigen epitope. Furthermore, the results show that to provide specificity the avoidance of unfavorable electrostatic interactions augments shape complementarity.

The docking procedure presented here successfully screens a very large number ($\approx 10^{10}$) of possible binding geometries to a reasonable number (≈ 50) of predicted complexes using the native structures of the proteins. For such a small number of candidates, it is possible to use more computationally demanding techniques to refine further the few remaining complexes to account for desolvation and, more importantly, conformational changes. Unless the interfacial side-chains are correctly positioned, true molecular recognition will not be achieved. Inclusion of a method for induced binding effects could lead to a general solution to the protein–protein docking problem.

Methods

Distance filtering

Distance filtering is implemented as a two-step process. First, a rapid check of intermolecular C^{α} distances between constraint residues is performed. For example, in the case of an antibody–antigen binding where the epitope is unknown, the C^{α} distances between residues in the hypervariable loops and all antigen residues would be checked. If a pair of C^{α} atoms is within a cutoff distance, in this case the sum of the side-chain lengths for the two residues (see legend to Table 2), the distances between all atoms of the two residues are checked. If any atom pair is within 4.5 Å then the distance constraint is satisfied. Predicted complexes that do not satisfy the distance constraint are discarded.

Global search and local refinement

A complete docking experiment consists of two distinct phases: global search and local refinement. It should be noted that high-resolution grids are used in both phases, unlike previous studies (Katchalski-Katzir *et al*., 1992; Vakser & Aflalo, 1994; Meyer *et al*., 1996) in which smaller, low-resolution grids were used during the global search. It is possible for us to use a high-resolution grid for both the initial search and the refinement due to the speed afforded by multiprocessing (see Technical information, below). The global search examines all translation (i.e. within the discrete space of the grid) and rotation space. This produces ($128^3 \times 6385$) $\approx 10^{10}$ possible docking geometries. Obviously, geometries with zero or negative correlation scores can be excluded immediately. However, several hundred thousand possible docking geometries still remain. To reduce the number of possibilities to manageable levels, only three complexes from each translational scan are saved to the ''stack''; those with the highest surface correlation scores and favourable electrostatics. This leaves ($3 \times 6385 =$)19,155 possible complexes

after the global search. The stack is sorted and the best 4000 geometries are kept. These complexes are filtered on the basis of available biochemical information and those that pass through the filter undergo local refinement. Each predicted geometry is shifted (±5 Å in each direction) and rotated (±5° for each Euler angle) slightly and the highest scoring complex is saved. Electrostatics are not calculated during local refinement for two reasons. First, it doubles the computational time required for the refinement stage of docking. Second, the docked geometry does not change significantly during refinement. Consequently, electrostatic interaction will not change significantly. Tests performed using electrostatic correlation during refinement showed little or no improvement in the final results (data not shown). At the end of the local refinement stage of docking, the stack is filtered again and the remaining complexes with the highest surface correlation scores are considered reasonable docking predictions.

Calculating RMS deviation

The quality of docking predictions is assessed by calculating the RMS deviation in the C^{α} atoms after superposition (Kabsch, 1978) of the predicted complex onto the crystal complex. Both receptor and ligand C^{α} coordinates are used during the superposition. The peptide backbone and amino acid side-chains undergo conformational changes upon binding. However, induced binding affects the side-chains more drastically than the main chain. So to avoid masking otherwise good results, side-chain atoms are excluded when calculating RMS deviations. In addition to total C^{α} RMS values, the RMS of the interface C^{α} atoms is also determined. Residues with any atom within 10 Å of the opposite protein comprise the interface.

Test systems

The enzyme/inhibitor systems used in this study consist of the following crystal structures (with their PDB codes): (1) CGI, human pancreatic trypsin inhibitor (1hpt) (Hecht *et al*., 1992) bound to α -chymotrypsinogen (1chg) (Freer *et al*., 1970). The PDB code of the complex is 1cgi (Hecht *et al*., 1991). (2) CHO, ovomucoid (2ovo) (Bode *et al*., 1985) bound to α chymotrypsin (5cha) (Blevins & Tulinsky, 1985). The PDB code of the complex is 1cho (Fujinaga *et al*., 1987). (3) KAI, bovine pancreatic trypsin inhibitor (1bpi) bound to kallikrein A (2pka) (Bode *et al*., 1983). The PDB code of the complex is 2kai (Chen & Bode, 1983). (4) PTC, bovine pancreatic trypsin inhibitor (4pti) (Wlodawer *et al*., 1987) bound to trypsin (2ptn) (Fehlhemmer *et al*., 1977). The PDB code of the complex is 2ptc (Marquart *et al*., 1983). (5) SNI, chymotrypsin inhibitor 2 (2ci2) (McPhalen & James, 1987) bound to subtilisin (1sup). The PDB code of the complex is 2sni (McPhalen & James, 1988). (6) SIC, *Streptomyces* subtilisin inhibitor (2ssi) (Mitsui *et al*., 1979) bound to subtilisin (1sup). The PDB code of the complex is 2sic (Takeuchi *et al*., 1991).

The antibody/antigen systems used in this study consisted of the following F_{ab}s and F_vs bound to lysozyme (1lza) (Maenaka *et al*., 1995): (1) FDL, D1.3 F_{ab} (1vfa), complex (1fdl) (Fischmann *et al*., 1991). (2) MLC, D44.1 (F_v (1mlb), complex (1mlc) (Braden *et al*., 1994). (3) HFL, HyHel-5 F_{ab} (2hfl) (Sheriff *et al*., 1987). (4) HFM, HyHel-10 F_{ab} (3hfm) (Padlan *et al*., 1989). Unfortunately, native crystal structures for the antibody in 2hfl and 3hfm are not yet solved. So the bound forms of the F_{ab} are used in HFL and HFM docking. Only the F_v regions of 1mlb, 2hfl, and 3hfm were used during docking.

Technical information

The complete docking package, named FTDOCK, consists of approximately 3,500 lines of Fortran 77 and Perl 5.0 (Wall & Schwartz, 1991) code designed to run under the UNIX operating system. All docking experiments were carried out on an SGI Power Challenge symmetric-array multiprocessor with 12 R10000 CPUs. Parallel compiler directives as well as the LIBFFT parallel maths library (J.-P. Panziera, SGI Paris, France) containing the necessary FFT routines are used to maximize computational efficiency. A complete docking experiment including post-filtering requires approximately six hours of CPU time using eight processors simultaneously. Preprocessor commands in the source code allow compilation on serial workstations.

Acknowledgements

The authors thank Matthew Betts for his help in identifying suitable test cases for docking. R. M. J. is a fellow of the Lloyd's of London Tercentenary Foundation. H. A. G. is a fellow of the European Molecular Biology Organization.

References

Bernstein, F. C., Koetzle, T. F., Williams, G. J. B., Meyer, E. F., Brice, M. D., Rodgers, J. R., Kennard, O., Shimanovichi, T. & Tasumi, M. (1977). The protein data bank: a computer-based archival file for macromolecular structures. *J. Mol. Biol.* **112**, 535–542.

Blevins, R. A. & Tulinsky, A. (1985). The refinement and the structure of the dimer of alpha-chymotrypsin at 1.67-Å resolution. *J. Biol. Chem.* **260**, 4264–4275.

Bode, W., Chen, Z., Bartels, K., Kutzbach, C., Schmidt-Kastner, G. & Bartunik, H. (1983). Refined 2 ångstrom X-ray crystal structure of porcine pancreatic kallikrein a and a specific trypsin-like proteinase, crystallization and structure determination and crystallographic refinement and structure and its comparison with bovine trypsin. *J. Mol. Biol.* **164**, 237–282.

Bode, W., Epp, O., Huber, R., Laskowski, M., Jr & Ardelt, W. (1985). The crystal and molecular structure of the third domain of silver pheasant ovomucoid (OMSVP3). *Eur. J. Biochem.* **147**, 387–395.

Bracewell, R. N. (1990). Numerical transforms. *Science,* **248**, 697–704.

Braden, B. C., Souchon, H., Eisele, J.-L., Bentley, G. A., Bhat, T. N., Navaza, J. & Poljak, R. J. (1994). Three-dimensional structures of the free and the antigen-complexed F_{ab} form monoclonal anti-lysozyme antibody D44.1. *J. Mol. Biol.* **243**, 767–781.

Chen, Z. & Bode, W. (1983). Refined 2.5 Å X-ray crystal structure of the complex formed by porcine kallikrein a and the crystallization, patterson search, structure comparison with its components and with the bovine trypsin-pancreatic trypsin inhibitor complex. *J. Mol. Biol.* **164**, 283–311.

Cherfils, J., Duquerroy, S. & Janin, J. (1991). Protein protein recognition analyzed by docking simulation. *Proteins,* **11**, 271–280.

DesJarlais, R. L., Sheridan, R. P., Seibel, G. L., Dixon, J. S., Kuntz, I. D. & Venkataraghavan, R. (1988). Using shape complementarity as an initial screen in designing ligands for a receptor binding site of known three dimensional structure. *J. Med. Chem.* **31**, 722–729.

Dunbrack, R. L., Jr., Gerloff, D. L., Bower, M., Chen, X., Lichtarge, O. & Cohen, F. E. (1997). Meeting review; the second meeting on the critical assessment of techniques for protein structure prediction (CASP2), Asilomar, California, December 13–16, 1996. *Folding & Design,* **2**, R27–R42.

Edmonds, D. T., Rogers, N. K. & Sternberg, M. J. E. (1984). Regular representation of irregular charge distributions: Application to the electrostatic potentials of globular proteins. *Mol. Phys.* **52**, 1487–1494.

Fehlhemmer, H., Bode, W. & Huber, R. (1977). Chrystal structure of bovine trypsinogen at 1.8 Å resolution. II crystallographic refinement, refined crystal structure and comparison with bovine trypsin. *J. Mol. Biol.* **111**, 415–438.

Fischmann, T. O., Bentley, G. A., Bhat, T. N., Boulot, G., Mariuzza, R. A., Phillips, S. E. V., Tello, D. & Poljak, R. J. (1991). Crystallographic refinement of the three-dimensional structure of the D1.3-lysozyme complex at 2.5 Å resolution. *J. Biol. Chem.* **266**, 12915–12920.

Freer, S. T., Kraut, J., Robertus, J. D., Wright, H. T. & Xuong, N. H. (1970). Chymotrypsinogen, 2.5 angstroms crystal structure, comparison with alpha-chymotrypsin, and implications for zymogen activation. *Biochemistry,* **9**, 1997–2009.

Fujinaga, M., Sielecki, A. R., Read, R. J., Ardelt, W., Laskowski, M., Jr & James, M. N. G. (1987). Crystal and molecular structures of the complex of alpha-chymotrypsin with its inhibitor turkey ovomucoid third domain at 1.8 Å resolution. *J. Mol. Biol.* **195**, 397–418.

Gilson, M. K. & Honig, B. (1987). Calculation of electrostatic potentials in an enzyme active site. *Nature,* **330**, 84–86.

Gilson, M. K. & Honig, B. (1988). Calculation of the total electrostatic energy of a macro-molecyular system: solvation energies, binding energies, and conformational analysis. *Proteins,* **4**, 7–18.

Hecht, H. J., Szardenings, M., Collins, J. & Schomburg, D. (1991). Three-dimensional structure of the complexes between bovine chymotrypsinogen a and two recombinant variants of human pancreatic secretory trypsin inhibitor (Kazal type). *J. Mol. Biol.* **220**, 711–722.

Hecht, H. J., Szardenings, M., Collins, J. & Schomburg, D. (1992). Three-dimensional structure of a recombinant variant of human pancreatic secretory trypsin inhibitor (Kazal type). *J. Mol. Biol.* **225**, 1095–1103.

Helmer-Citterich, M. & Tramontano, A. (1994). Puzzle: a new method for automated protein docking based on surface shape complementarity. *J. Mol. Biol.* **235**, 1021–1031.

Hingerty, B. E., Ritchie, R. H., Ferrell, T. L. & Turner, J. E. (1985). *Biopolymers,* **24**, 427.

Jackson, R. M. & Sternberg, M. J. E. (1995). A continuum model for protein/protein interactions: application to the docking problem. *J. Mol. Biol.* **250**, 258–275.

Janin, J. (1995a). Protein–protein recognition. *Prog. Biophys.Mol. Biol.* **64**, 145–166.

Janin, J. (1995b). Elusive affinities. *Proteins,* **21**, 30–39.

Jiang, F. & Kim, S. (1991). Soft docking matching of molecular surface cubes. *J. Mol. Biol.* **219**, 79–102.

Kabsch, W. (1978). A discussion of the solution for the best rotation to relate two sets of vectors. *Acta Crystallog. sect. A,* **34**, 827–828.

Katchalski-Katzir, E., Shariv, I., Eisenstein, M., Friesen, A. A., Aflalo, C. & Wodak, S. J. (1992). Molecular surface recognition: Determination of geometric fit between proteins and their ligands by correlation techniques. *Proc. Natl. Acad. Sci. USA,* **89**, 2195–2199.

Kuntz, I. D., Blaney, J. M., Oatley, S. J., Langridge, R. & Ferrin, T. E. (1982). A geometric approach to macromolecule-ligand interactions. *J. Mol. Biol.* **161**, 269–288.

Laskiwski, R. A. (1995). Surfnet: A program for visualizing molecular surfaces, cavities, and intermolecular interactions. *J. Mol. Graph.* **13**, 323–330.

Laskowski, R. A., Luscombe, N. M., Swindells, M. B. & Thornton, J. M. (1996). Protein clefts in molecular recognition and function. *Protein Sci.* **5**, 2438–2452.

Lattman, E. E. (1972). Optimal sampling of the rotation function. In *The Molelcular Replacement Method* (Rossman, M. G., ed.), pp. 179–185, Gordon and Breach, New York.

Lawrence, M. C. & Colman, P. M. (1993). Shape complementarity at protein/protein interfaces. *J. Mol. Biol.* **234**, 946–950.

MacCullum, R. M., Martin, A. C. R. & Thornton, J. M. (1996). Protein–protein recognition. *J. Mol. Biol.* **262**, 732–745.

Maenaka, K., Matsushima, M., Song, H., Sunada, F., Watanabe, K. & Kumagai, I. (1995). Dissection of protein–carbohydrate interactions in mutant hen egg-white lysozyme complexes and their hydrolytic activity. *J. Mol. Biol.* **247**, 281–293.

Marquart, M., Walter, J., Deisenhofer, J., Bode, W. & Huber, R. (1983). The geometry of the reactive site and of the peptide groups in trypsin and trypsinogen and its complexes with inhibitors. *Acta Crystallog.* **39**, 480.

McPhalen, C. A. & James, M. N. G. (1987). Crystal and molecular structure of the serine proteinase inhibitor ci-2 from barley seeds. *Biochemistry,* **26**, 261–269.

McPhalen, C. A. & James, M. N. G. (1988). Structural comparison of two serine proteinase-protein inhibitor complexes, eglin-c-subtilisin Carlsberg and CI-2-subtilisin novo. *Biochemistry,* **27**, 6582–6589.

Meyer, M., Wilson, P. & D., S. (1996). Hydrogen bonding and molecular surface shape complementarity

as a basis for protein docking. *J. Mol. Biol.* **264**, 199–210.
Mitsui, Y., Satow, Y., Watanabe, Y. & Iitaka, Y. (1979). Crystal structure of a bacterial protein proteinase inhibitor (streptomyces subtilisin inhibitor) at 2.6 Å resolution. *J. Mol. Biol.* **131**, 697–724.
Nicholls, A. & Honig, B. (1991). A rapid finite difference algorithm, utilizing successive over-relaxation to solve the Poisson-Boltzmann equation. *J. Comput. Chem.* **12**, 435–445.
Norel, R., Lin, S. L., Wolfson, H. L. & Nussinov, R. (1995). Molecular surface complementarity at protein–protein interfaces: the critical role played by surface normals at well placed sparse points in docking. *J. Mol. Biol.* **252**, 263–273.
Padlan, E. A., Silverton, E. W., Sheriff, S., Cohen, G. H., Smith-Gill, S. J. & Davies, D. R. (1989). Structure of an antibody-antigen complex. crystal structure of the HyHEL-10 F_{ab}-lysozyme complex. *Proc. Natl Acad. Sci. USA,* **86**, 5938–5942.
Press, W. H., Teukolsky, S. A., Vetterling, W. T. & Flannery, B. P. (1986). *Numerical Recipes in Fortran,* Cambridge University Press, Cambridge.
Ptitsyn, O. B. (1995). Structures of folding intermediates. *Curr. Opin. Struct. Biol.* **5**, 74–78.
Rogers, N. K. & Sternberg, M. J. E. (1984). Electrostatic interactions in globular proteins: Different dielectric models applied to the packing of α-helices. *J. Mol. Biol.* **174**, 527–542.
Sharp, K. & Honig, B. (1990). Electrostatic interactions in macromolecules: theory and applications. *Annu. Rev. Biophys. Biophys. Chem.* **19**, 301–332.
Sheriff, S., Silverton, E. W., Padlan, E. A., Cohen, G. H., Smith-Gill, S. J. & Davies, D. R. (1987). Three-dimensional structure of an antibody-antigen complex. *Proc. Natl Acad. Sci. USA,* **84**, 8075–8079.
Shoichet, B. K. & Kuntz, I. D. (1991). Protein docking and complementarity. *J. Mol. Biol.* **221**, 327–346.
Shoichet, B. K. & Kuntz, I. D. (1996). Predicting the structure of protein complexes: a step in the right direction. *Chem. Biol.* **3**, 151–156.
Strynadka, N. C. J., Eisenstein, M., Katchalski-Katzir, E., Shoichet, B. K., Kuntz, I. D., Abagyan, R., Totrov, M., Janin, J., Cherfils, J., Zimmerman, F., Olson, A., Duncan, B., Rao, M., Jackson, R., Sternberg, M. J. E. & James, M. N. G. (1996). Molecular docking programs successfully predict the binding of a β-lactamese inhibitory protein to TEM-1 β-lactamese. *Nature Struct. Biol.* **3**, 233–239.
Takechi, Y., Satow, Y., Nakamura, K. T. & Mitsui, Y. (1991). Refined crystal structure of the complex of subtilisin BPN′ and streptomyces subtilisin inhibitor at 1.8 Å resolution. *J. Mol. Biol.* **221**, 309–325.
Totrov, M. & Abagyan, R. (1994). Detailed ab initio prediction of lysozyme-antibody complex with 1.6 Å accuracy. *Nature Struct. Biol.* **1**, 259–263.
Vakser, I. A. & Aflao, C. (1994). Hydrophobic docking: a proposed enhancement to molecular recognition techniques. *Proteins,* **20**, 320–329.
Wall, L. & Schwartz, R. L. (1991). *Programming Perl* O'Reilly & Associates, Inc., Sebastopol, CA.
Walls, P. H. & Sternberg, M. J. E. (1992). New algorithm to model protein–protein recognition based on surface complementarity. *J. Mol. Biol.* **228**, 277–297.
Warwicker, J. & Watson, H. C. (1982). Calculation of the electric potential in the active site cleft due to α-helix dipoles. *J. Mol. Biol.* **157**, 671–679.
Weng, Z. P., Vajda, S. & Delisi, C. (1996). Prediction of protein complexes using empirical free-energy functions. *Protein Sci.* **5**, 614–626.
Wlodawer, A., Deisenhofer, J. & Huber, R. (1987). Comparison of two highly refined structures of bovine pancreatic trypsin inhibitor. *J. Mol. Biol.* **193**, 145–156.

Edited by J. Thornton

(Received 3 March 1997; received in revised form 21 March 1997; accepted 7 June 1997)

Note added in proof: For availability of the program FTDOCK please see our home page (http://www.icnet.uk/bmm) or contact M. J. E. S. at m.sternberg@icrf.icnet.uk.